Individual differences in associative memory among older adults explained by hippocampal subfield structure and function

Valerie A. Carr[a,1], Jeffrey D. Bernstein[b], Serra E. Favila[a], Brian K. Rutt[c], Geoffrey A. Kerchner[b], and Anthony D. Wagner[a,d]

[a]Department of Psychology, Stanford University, Stanford, CA 94305; [b]Department of Neurology and Neurological Sciences, Stanford University, Stanford, CA 94305; [c]Department of Radiology, Stanford University, Stanford, CA 94305; and [d]Stanford Neuroscience Institute, Stanford University, Stanford, CA 94305

Edited by James L. McGaugh, University of California, Irvine, CA, and approved August 22, 2017 (received for review July 31, 2017)

Older adults experience impairments in episodic memory, ranging from mild to clinically significant. Given the critical role of the medial temporal lobe (MTL) in episodic memory, age-related changes in MTL structure and function may partially account for individual differences in memory. Using ultra–high-field 7T structural MRI and high-resolution 3T functional MRI (hr-fMRI), we evaluated MTL subfield thickness and function in older adults representing a spectrum of cognitive health. Participants performed an associative memory task during hr-fMRI in which they encoded and later retrieved face–name pairs. Motivated by prior research, we hypothesized that differences in performance would be explained by the following: (*i*) entorhinal cortex (ERC) and CA1 apical neuropil layer [CA1–stratum radiatum lacunosum moleculare (SRLM)] thickness, and (*ii*) activity in ERC and the dentate gyrus (DG)/CA3 region. Regression analyses revealed that this combination of factors significantly accounted for variability in memory performance. Among these metrics, CA1-SRLM thickness was positively associated with memory, whereas DG/CA3 retrieval activity was negatively associated with memory. Furthermore, including structural and functional metrics in the same model better accounted for performance than did single-modality models. These results advance the understanding of how independent but converging influences of both MTL subfield structure and function contribute to age-related memory impairment, complementing findings in the rodent and human postmortem literatures.

episodic memory | hippocampus | aging | mild cognitive impairment | Alzheimer's disease

Episodic memory, or the capacity to encode and subsequently retrieve memories for events, is known to be particularly vulnerable to age-related change (1–3). Older adults show varying degrees of episodic memory impairment, ranging from mild to clinically significant. One potential factor underlying such differences is variability in the structure and function of the medial temporal lobe (MTL).

The MTL is essential for episodic memory (4–7), and research across species indicates that the MTL changes in both healthy aging and in age-related neurodegenerative disease (for reviews, see refs. 8 and 9). Critically, however, the MTL is not a unitary structure. Rather, it is composed of multiple regions with differing anatomy and connectivity (see, e.g., ref. 10), including subfields of the hippocampal formation [CA1, CA2, CA3, dentate gyrus (DG), and subiculum], and the entorhinal (ERC), perirhinal (PRC), and parahippocampal (PHC) cortices (Fig. 1*A*). Moreover, evidence in rodents and humans suggests that these subfields are differentially affected by age, as well as by age-related disease (8, 9, 11).

Converging evidence in human studies of healthy aging using high-resolution magnetic resonance imaging (MRI) suggests disproportionate age-related atrophy in CA1 (12–15), although some studies point to selective atrophy of the subiculum or DG/CA3, while others suggest changes encompassing multiple subfields (for a review, see ref. 11). Studies examining age-related changes in MTL cortex suggest that anterior portions of the parahippocampal gyrus, including ERC, are particularly susceptible (15–19).

Beyond healthy aging, postmortem studies demonstrate that ERC and CA1 are among the first regions to show preclinical Alzheimer's disease (AD) pathology (20–22). Similarly, in vivo imaging studies of patients with mild cognitive impairment (MCI) (a clinical precursor to AD) and mild AD demonstrate focal atrophy in ERC (23–25) and CA1 (e.g., ref. 26), although some studies demonstrate targeted atrophy of subiculum or broader atrophy in multiple hippocampal subfields (11).

Histological studies show that the earliest appearance of AD pathology in CA1 is in the stratum radiatum and stratum lacunosum moleculare (SRLM) (20, 22). Motivated by these findings, researchers have begun using ultra–high-field 7T MRI to examine layer-specific CA1 atrophy in vivo. Results demonstrate thinning of CA1-SRLM in patients with mild AD (27), as well as in healthy older adults relative to younger adults (28). Taken together, findings in both healthy aging and in mild AD suggest a similar pattern of atrophy targeting ERC and CA1. The precise relationship between such changes in MTL subfield structure and changes in episodic memory performance remains underspecified, however.

In addition to structure, age-related changes in MTL function may also contribute to episodic memory decline. Functional

Significance

Older adults differ in the degree to which they experience memory impairments, but the underlying factors contributing to this variability remain unclear. Motivated by the essential role of the medial temporal lobe (MTL) in declarative memory, we investigated whether episodic memory differences among older adults can be explained by differences in MTL subfield structure and function. Using high-resolution magnetic resonance imaging, we demonstrated that a combination of structural and functional subfield measures significantly accounted for differences in memory performance. These findings advance understanding of how independent but converging influences of both MTL structure and function contribute to age-related impairment in episodic memory, complementing findings in the rodent and human postmortem literatures.

Author contributions: V.A.C., G.A.K., and A.D.W. designed research; V.A.C., J.D.B., and S.E.F. performed research; B.K.R. contributed new reagents/analytic tools; V.A.C., J.D.B., and S.E.F. analyzed data; and V.A.C., G.A.K., and A.D.W. wrote the paper.

The authors declare no conflict of interest.

This article is a PNAS Direct Submission.

Data deposition: The human MRI data reported in this paper have been deposited in the Stanford Digital Repository (SDR), https://purl.stanford.edu/dm781xs5457.

[1]To whom correspondence should be addressed. Email: valerie.carr@sjsu.edu.

This article contains supporting information online at www.pnas.org/lookup/suppl/doi:10.1073/pnas.1713308114/-/DCSupplemental.

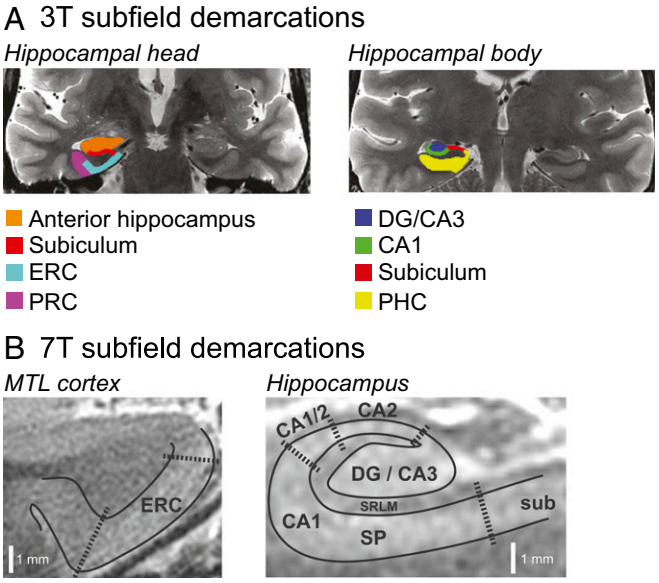

Fig. 1. Sample MTL subfield demarcations. (*A*) Subfields used in 3T functional analyses. (*B*) Layer-specific subfields used in 7T structural analyses. DG, dentate gyrus; ERC, entorhinal cortex; MTL, medial temporal lobe; PHC, parahippocampal cortex; PRC, perirhinal cortex; SP, stratum pyramidale; SRLM, stratum radiatum lacunosum moleculare.

MRI (fMRI) studies of healthy aging demonstrate inconsistent findings, with some studies revealing decreased MTL activity, and others showing increased activity or no differences in activity with age (for a review, see ref. 29). Although many differences exist between studies, a likely factor contributing to their divergent findings is the relatively low spatial resolution used. If individual subfields are differentially vulnerable to age-related change, then averaging activity across regions could produce variable findings. Importantly, research in aged rodents suggests focal changes, indicating selective synaptic weakening among perforant path inputs from ERC to DG and CA3, as well as representational rigidity in CA3 place cells (8, 9, 11).

In humans, researchers have begun using high-resolution fMRI (hr-fMRI) (30) to test focal predictions from the rodent literature. For example, recent studies of item recognition memory reveal increased DG/CA3 activity in healthy older relative to younger adults (31), and activity patterns in DG/CA3 in older adults that demonstrate a form of representational rigidity (32). Similarly, other studies have shown DG/CA3 hyperactivity in individuals with MCI relative to healthy controls using the same item recognition task (33) and further indicate that pharmacologically reducing this activity leads to improved task performance (34, 35).

The degree to which age-related changes in MTL cortical function are focal or widespread is unclear, given that few hr-fMRI studies have documented such changes. Yassa et al. (33) recently reported decreased ERC activity in individuals with MCI, but this finding is at odds with several standard-resolution fMRI studies reporting increased activity along the parahippocampal gyrus—particularly anterior regions encompassing ERC—in older relative to younger adults (36–39), as well as in older adults with high levels of amyloid deposition (40) or with increased genetic risk of developing AD (41).

Critically, no study to date has integrated high-resolution metrics of both MTL subfield structure and function to determine the relative influence of these measures on episodic memory. In the current study, we used ultra–high-field 7T structural MRI and hr-fMRI at 3 T in older adults to determine whether individual differences in episodic memory can be explained by a combination of subfield and layer-specific metrics of MTL structure and function. To allow for sufficient differences across individuals in memory performance, participants included healthy older adults as well as those experiencing subjective cognitive impairment (SCI) or amnestic mild cognitive impairment (aMCI).

Given the key role of the hippocampus in associative memory (e.g., refs. 6 and 42) and reports of differential age-related impairments in associative relative to item memory (e.g., ref. 3), participants underwent hr-fMRI while performing an associative memory task (Fig. 2). We aimed to determine whether variability in associative memory performance could be explained by variability in a specific combination of structural and functional metrics. Based on prior structural findings, we hypothesized that ERC (15–19) and CA1-SRLM (11, 28) thickness would be positively linked to associative memory performance. Motivated by prior functional findings, we hypothesized that task-related activity in DG/CA3 (31, 33–35) and ERC (36–41) would be negatively linked to associative memory performance. Finally, we hypothesized that this combination of structural and functional metrics would better account for individual differences in associative memory performance than structural or functional measures alone.

Results

The present multimodal study yielded a number of different measures. We briefly present findings from each modality, and then report our main analyses relating the combination of these measures to memory performance.

Behavioral Results. Concurrent with fMRI, participants performed an associative memory task (Fig. 2). Participants first viewed face–name pairs and then performed a recognition test in which they discriminated between three face–name pair types: intact, recombined, and novel. From the recognition test data, we calculated a sensitivity index, associative d', which served as the metric of associative memory performance used in our regression analyses. Variability across participants for this measure is demonstrated in Fig. 2 (see Fig. S1*A* for response rates broken down by condition and Fig. S1*B* for variability in item d').

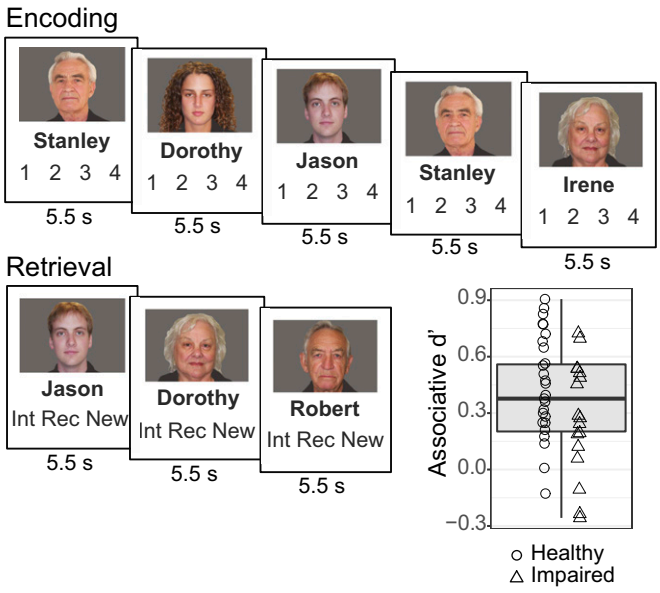

Fig. 2. Associative memory paradigm and results. During encoding, participants subjectively rated how well each name fit its associated face on a scale from 1 to 4. During retrieval, participants made judgments regarding whether a given face–name pair was intact, recombined, or new. Box plot demonstrates individual differences in task performance as measured by associative d'.

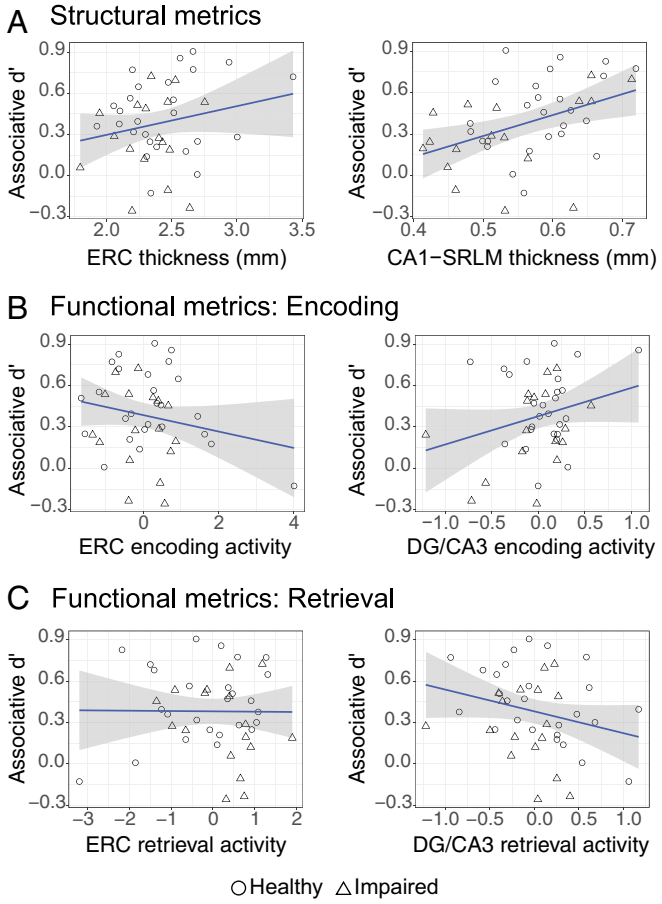

Fig. 3. Relationship between associative memory performance and measures of MTL subfield structure and function. All plots represent raw data. (*A*) Scatter plots showing relationship between bilateral ERC or bilateral CA1-SRLM thickness and associative *d′*. (*B*) Scatter plots showing relationship between bilateral ERC or bilateral DG/CA3 activity associated with successful encoding and associative *d′*. (*C*) Scatter plots showing relationship between bilateral ERC or bilateral DG/CA3 activity associated with retrieval success and associative *d′*. DG, dentate gyrus; ERC, entorhinal cortex; MTL, medial temporal lobe; SRLM, stratum radiatum lacunosum moleculare.

7T Structural Results. Analyses of structural data focused on our a priori regions of interest (ROIs), ERC and CA1-SRLM. We assessed the relationship between subfield thickness and associative *d′* using separate regression models for each ROI while controlling for group and age (see Fig. 3*A* for scatter plots of the raw data). Results demonstrate that although ERC thickness did not significantly account for variability in memory performance ($P > 0.3$), CA1-SRLM thickness was positively associated with memory ($\beta = 0.092$, $P = 0.048$). See *SI Results* and Fig. S2*A* for analyses of non-a priori ROIs, including significant findings for the CA1 stratum pyramidale, or SP, layer.

3T Functional Results. Analyses of functional data focused on encoding and retrieval activity in our a priori ROIs, ERC and DG/CA3 (see *SI Results* and Fig. S2 *B* and *C* for analyses in additional subfields). Encoding activity for each ROI was defined as follows: [subsequently intact trials called "intact" (SII)] − [subsequently intact trials called "recombined" (SIR)]. See *SI Methods* and Fig. S3 for a complementary analysis of encoding activity according to stimulus novelty (novel − repeat). Retrieval activity was defined as: [intact trials called intact (II)] − [intact trials called recombined (IR)]. Next, for each ROI, we assessed the relationship between functional activity and associative *d′* separately for encoding and retrieval while controlling for group and age (see Fig. 3 for scatter plots of the raw data). At encoding, results demonstrate that neither ERC activity nor DG/CA3 activity significantly explained variance in task performance (values of $P > 0.1$). At retrieval, DG/CA3 activity was negatively associated with memory ($\beta = -0.118$, $P = 0.007$), whereas ERC activity did not significantly account for variability in memory performance ($P > 0.7$). See Fig. S4 for retrieval activity broken down by condition in each ROI.

Multiple Linear Regression. We next examined whether the combination of our a priori structural and functional metrics could significantly account for variability in associative *d′* when controlling for group and age. Separate regression analyses were performed for encoding and retrieval, such that, for each analysis, structural and control variables remained the same, but functional metrics were specific to task phase.

The encoding model significantly accounted for variability in memory performance [$F_{(6,36)} = 2.569$, $P = 0.036$, adjusted $R^2 = 0.183$], but the only subfield metric approaching significance was CA1-SRLM thickness, which demonstrated a trend for a positive association with memory performance (Table 1). This pattern of significance did not differ when excluding an ERC thickness outlier or separate ERC activity and DG/CA3 activity outliers (outliers defined as >2 SDs from the mean). See Table S1 for results from a complementary encoding model using activity associated with stimulus novelty.

The retrieval model also significantly explained variability in associative memory performance [$F_{(6,36)} = 5.086$, $P < 0.001$, adjusted $R^2 = 0.369$]. This model revealed that two subfield metrics were significantly linked to performance: CA1-SRLM thickness, which was positively associated with memory, and DG/CA3 retrieval activity, which was negatively associated with memory (Table 1). This pattern of significance did not differ when excluding an ERC thickness outlier or separate ERC activity and DG/CA3 activity outliers.

Next, we performed three follow-up analyses pertaining to the retrieval model. First, to mitigate concerns regarding the large age range in our sample, we repeated the analysis using participants aged 60 and above, the results of which were similar to the model including all participants (*SI Results* and Table S2). Second, we examined whether the same explanatory variables could account for performance on a different test of episodic memory by

Table 1. Regression model results

Model	Variable	β	SE	*P*
Encoding	ERC thickness	0.019	0.047	0.688
	CA1-SRLM thickness	0.085	0.048	0.087~
	ERC activity	−0.056	0.043	0.204
	DG/CA3 activity	0.070	0.044	0.123
	Group	0.015	0.045	0.287
	Age	−0.049	0.045	0.739
Retrieval	ERC thickness	0.003	0.040	0.946
	CA1-SRLM thickness	0.136	0.044	0.004**
	ERC activity	−0.002	0.038	0.947
	DG/CA3 activity	−0.155	0.040	<0.001***
	Group	0.063	0.039	0.111
	Age	−0.072	0.038	0.065~
Structure only	ERC thickness	0.014	0.046	0.766
	CA1-SRLM thickness	0.086	0.049	0.088~
	Group	0.055	0.044	0.226
	Age	−0.044	0.044	0.314
Function only	ERC activity	−0.001	0.041	0.968
	DG/CA3 activity	−0.118	0.042	0.008**
	Group	0.099	0.042	0.022*
	Age	−0.100	0.041	0.021*

DG, dentate gyrus; ERC, entorhinal cortex; SRLM, stratum radiatum lacunosum moleculare. ~$P < 0.1$, *$P < 0.05$, **$P < 0.01$, ***$P < 0.001$.

PSYCHOLOGICAL AND COGNITIVE SCIENCES

modifying the dependent variable to be a composite measure of neuropsychological tests of episodic memory (*SI Methods*). This model significantly accounted for variability in memory, with CA1-SRLM thickness being positively associated with memory performance (*SI Results* and Table S2). Third, we evaluated the degree to which whole hippocampal structure and function were associated with associative d'. Findings for this model paralleled those of the subfield-specific model, with hippocampal area showing a positive association with memory and retrieval activity showing a negative association with memory (*SI Results* and Table S2).

Model Comparison. Focusing on retrieval, we next evaluated whether our model inclusive of both structural and functional measures better explains variability in memory than a model with structural or functional measures alone (with each model controlling for group and age). Results of each model can be found in Table 1: structure-plus-function model: $F_{(6,\ 36)} = 5.086$, $P < 0.001$, adjusted $R^2 = 0.369$; structure-only model: $F_{(4,38)} = 2.762$, $P = 0.041$, adjusted $R^2 = 0.144$; function-only model: $F_{(4,38)} = 3.863$, $P = 0.010$, adjusted $R^2 = 0.214$. Next, we compared these models as follows (*i*): structure plus function compared with structure only, and (*ii*) structure plus function compared with function only. The structure-plus-function model accounted for significantly more of the variance in associative d' than either structure only [$F_{(2,36)} = 7.768$, $P = 0.002$] or function only [$F_{(2,36)} = 5.644$, $P = 0.007$].

Group Differences. For complementary analyses evaluating group differences in each modality (behavior, structure, and function) rather than individual differences, see *SI Results*.

Discussion

While numerous studies point to episodic memory decline with age (1–3), substantial differences exist in the degree to which individuals exhibit memory impairment. Using a combination of ultra–high-field 7T structural MRI and 3T hr-MRI, we examined whether individual differences in episodic memory among older adults can be explained, in part, by differences in MTL subfield structure and function. Supporting this hypothesis, our analyses demonstrated that variability in hippocampal structure and function partially accounts for variability in memory performance. Specifically, CA1-SRLM thickness is positively linked to performance and DG/CA3 retrieval activity is negatively linked to performance. Moreover, combining structural and functional metrics better explained variability in memory performance than did single-modality models. Although prior aging studies have examined independent contributions of MTL subfield structure or function to memory (e.g., refs. 31–33 and 43–45), here we incorporated both modalities and demonstrated independent but converging influences on performance.

Extensive evidence indicates that the MTL is vulnerable to atrophy in both putatively healthy aging and in age-related disease (46). Aside from the five million Americans with clinically manifest AD (47), many more harbor neuropathological signs of the disease. By some estimates, AD biomarkers may be present two decades before a diagnosis is made (48). In a large autopsy series, for example, early stage neurofibrillary tau pathology was evident in the MTL in over 60% of 60-y-olds (49). Tau pathology is remarkably focal early in AD, first affecting portions of ERC and CA1. In CA1, postmortem studies show that pathology first appears in the SRLM layer (20, 50, 51), and in vivo work from our group demonstrates that, within CA1, SRLM is selectively vulnerable to atrophy in mild AD relative to controls (ref. 27; see also, ref. 52), as well as in healthy older relative to younger adults (28). Along with the current data, these postmortem and imaging findings raise the possibility that putatively healthy individuals with a thin CA1-SRLM are experiencing early-stage AD-related tau pathology that contributes to poor memory performance.

ERC is also implicated in age-related atrophy (15–19) and is an early target of AD pathology. Our results, however, did not indicate a significant relationship between ERC thickness and memory performance. Although the MTL is known to support associative memory, the hippocampus is thought to play a more critical role in binding together and subsequently pattern completing elements of an event than MTL cortex, which is hypothesized to differentially support item recognition (42). As such, future studies should investigate the degree to which age-related differences in ERC structure differentially explain performance on item vs. associative tests of memory.

Our structural analyses focused on ERC and CA1-SRLM based upon prior findings (11, 15–19, 28) as well as the need to avoid overfitting our regression models. However, supplemental analyses revealed that CA1-SP thickness also was positively associated with performance. This finding extends prior work from our laboratory demonstrating positive correlations between both layers of CA1 and memory in mild AD (45), as well as other research showing a relationship between atrophy of CA1 and memory impairment in individuals with MCI (43, 44). Although some studies of aging and mild AD have reported selective atrophy of DG/CA3 or subiculum (11), our supplemental analysis of DG/CA3 area revealed nonsignificant findings, and we did not measure subiculum size in this study. Future large-scale studies with a sample size sufficient to evaluate each subfield's contributions to memory in a single model may further resolve discrepancies in the literature.

In addition to clarifying the relationship between subfield structure and memory, we also sought to examine whether differences in subfield function can partially account for memory performance. Our findings indicate a negative relationship between retrieval activity in DG/CA3 and associative memory performance, such that greater activity during successful retrieval is associated with worse task performance. These results support prior findings demonstrating DG/CA3 hyperactivity in older relative to younger adults (31) and individuals with MCI relative to controls (33–35) during a test of item recognition. Here, we extend these findings to demonstrate that increased DG/CA3 activity is linked to poor performance during associative recognition, a type of memory thought to be more vulnerable to age-related change than item memory (e.g., ref. 3). Our results are also in agreement with standard-resolution studies of associative memory that demonstrate hippocampal hyperactivity during successful memory trials in individuals with MCI relative to controls (53). It bears noting, however, that other standard-resolution studies report a positive relationship between hippocampal retrieval activity and associative memory performance across the life span (see, e.g., ref. 54). Given that averaging activity across subfields may produce variable findings, continued high-resolution investigation of hippocampal function may help to resolve such inconsistencies.

One possible explanation for the consistent finding of increased hippocampal, and particularly DG/CA3, activity in older adults during memory success is that it is a form of neural compensation. However, given that many older adults exhibit tau pathology in the absence of an AD diagnosis (49), an alternate explanation for this hyperactivity is hippocampal excitotoxicity associated with AD pathology (55, 56). Alternatively, findings in aged rodents indicate that memory deficits associated with hippocampal hyperactivity may result from dysfunction of inhibitory interneurons (8, 9). Taken together, these findings suggest that DG/CA3 hyperactivity negatively affects memory performance, but the underlying mechanisms of this increased activity remain underspecified. It bears noting that supplemental analyses also revealed a trend for a negative relationship between memory and retrieval activity in CA1 and subiculum. Future large-scale studies should include activity from multiple hippocampal subfields in the same model to help to determine the relative explanatory power of each subfield's activity.

Outside of the hippocampus, ERC has also been implicated in age-related dysfunction (33, 36–41); our findings, however, were not significant. As with ERC structure, it will be beneficial for future studies to examine the relationship between ERC function and performance on tests of item vs. associative memory. Additionally, given that our imaging protocol was limited to the MTL, future whole-

brain studies are needed to determine whether and how structural and functional differences in prefrontal and parietal regions explain differences in episodic memory.

Importantly, rather than independently consider the relationship of MTL subfield structure or function with memory performance, we combined measures from both modalities into a single model. This combined model explained significantly more of the variance in memory performance than one inclusive of structural or functional measures alone. This study is a demonstration of independent but converging influences of MTL subfield structure and function on episodic memory in older adults. These results complement prior findings in the rodent and human postmortem literatures demonstrating subfield-specific changes with age, and provide an important bridge to understanding how these changes influence human behavior in vivo.

Methods

Participants. Sixty-one older adults (51–85 y) participated in the study. Four were dropped from analysis due to poor quality 7T structural images, seven were dropped due to excessive motion during 3T functional scans, and seven were dropped due to performance that yielded insufficient trial numbers (<10) for at least one condition of interest in the fMRI analyses. Thus, results reported here focus on the remaining 43 participants with a full dataset. Of these, 26 were healthy older adults (16 female, 2 left-handed), and 17 were patients with cognitive impairment (4 female, 1 left-handed). See Table S3 for detailed characteristics of each group and *SI Methods* for a description of our clinical assessment and diagnostic criteria for all participants. All study metrics, including clinical assessment, 7T imaging, and 3T imaging, were acquired within an average window of 68.2 d (range, 2–185 d; SD, 6.2 d). All participants provided informed consent in accordance with a protocol approved by the Stanford Institutional Review Board.

Materials. MATLAB Psychophysics Toolbox was used for stimulus presentation and response collection. Stimuli included 140 color photos of unfamiliar faces paired with 140 fictional first names. Faces were drawn from the Center for Vital Longevity Face Database (agingmind.utdallas.edu/download-stimuli/face-database/) and modified by Ebner (57) to neutralize clothing and background. The pictured individuals were Caucasian, ranged in age from 18–94 y, and had a neutral expression. Names were drawn from the Social Security Administration's database of popular baby names (www.ssa.gov/OACT/babynames/) from the 1920s to the 1980s.

Behavioral Procedure.

Stimulus presentation. Concurrent with fMRI, participants performed an associative memory task consisting of encoding and retrieval phases (Fig. 2). During encoding, participants viewed face–name pairs and made a subjective decision as to how well each name fit the corresponding face (adapted from ref. 58), a strategy designed to augment associative encoding. Participants practiced the encoding task before entering the scanner; four of these practice pairs then appeared repeatedly during encoding (but not retrieval) to allow for comparison of activity during novel and repeat trials. Encoding was divided across four functional runs, each consisting of 26 novel and 6 repeated face–name trials (duration, 5.5 s) interspersed with fixation trials (duration, 0.5–12.5 s). Following encoding, participants performed an associative recognition memory test in which they were presented with three face–name pair types: intact, recombined, and novel (duration, 5.5 s), and made one of three responses: intact, recombined, or novel. The retrieval phase spanned four functional runs, each consisting of 18 intact, 8 recombined, and 8 novel trials interspersed with fixation trials (duration, 0.5–12.5 s). Trial order for all runs was determined using optseq (surfer.nmr.mgh.harvard.edu/optseq/).

Response classification. Recognition test results were used to classify retrieval trials into each of nine conditions (3 pair types × 3 responses). Here, we abbreviate trial types with two letters such that the first letter refers to the pair type and the second letter to the response. IR, for example, would serve as the abbreviation for intact pairs (I) incorrectly identified as recombined (R). Recognition test results were also used to backsort encoding trials into each of four conditions: subsequently intact pairs called intact (SII), subsequently intact pairs called recombined (SIR), subsequently intact pairs called "novel" (SIN), and subsequently recombined pairs (SR). SR trials could not be broken down by performance because each member of the encoding pair was then recombined into separate trials.

Sensitivity index. For regression analyses, we chose a sensitivity index, associative d', as our metric of behavioral performance. Given that we were most interested in associative memory, hit rate was defined as the rate of correctly responding intact to intact pairs (II), and the false alarm rate was defined as the rate of incorrectly responding intact to recombined pairs (RI). Thus, our associative d' measure was as follows: $d' = Z(\text{II rate}) - Z(\text{RI rate})$. See *SI Methods* for discussion of complementary-item d' analyses.

7T Structural MRI.

Data acquisition. Participants were scanned on a 7T GE Discovery MR950 MRI scanner (GE Healthcare) using 2-channel transmit and a 32-channel radiofrequency receive-only head coil (Nova Medical). High-resolution oblique coronal images were acquired perpendicular to the long axis of the hippocampus using a T2-weighted fast spin echo sequence [repetition time (TR), cardiac gated, ∼5–6 s; echo time (TE), 49 ms; echo train length, 8; bandwidth, ±15.6 kHz; field of view (FOV), 17 cm; slice thickness, 1.5 mm; slice gap, 0.5 mm; 16 slices; matrix, 768 × 768; voxel size, 0.22 × 0.22 × 1.5 mm].

Data analysis. MTL subfield boundaries (Fig. 1*B*) and associated structural metrics were derived using previously described procedures (see ref. 45 and *SI Methods*). For each subfield, we averaged thickness across slices to yield one value per hemisphere per participant, and then averaged values across hemispheres to obtain a single metric for each subfield in each participant. Subfields were segmented by one rater (J.D.B.) blinded to group status.

3T fMRI.

Data acquisition. Data were acquired on a 3T GE Discovery MR750 MRI scanner (GE Healthcare) using a 32-channel radiofrequency receive-only head coil (Nova Medical). Functional data were acquired using an in-plane–accelerated echo-planar imaging (EPI) sequence (in-plane acceleration factor, 2) consisting of 27 oblique axial slices parallel to the long axis of the hippocampus (TR, 2 s; TE, 32 ms; FOV, 20 cm; voxel size, 1.67 × 1.67 × 1.5 mm). To correct for distortions of the B0 field that may occur with EPI imaging, we collected a B0 field map every second functional run with the same slice prescription as the functional runs (TR, 1 s; TE, 45 ms; FOV, 20 cm; voxel size, 0.89 × 0.89 × 1.5 mm; slices, 27). T2-weighted structural images were collected perpendicular to the long axis of the hippocampus to allow for subfield segmentation (TR, 4.2 s; TE, 68 ms; FOV, 22 cm; voxel size, 0.43 × 0.43 × 2 mm; slices, 29).

Data analysis. Preprocessing and analyses of functional data were performed using SPM8 (www.fil.ion.ucl.ac.uk/spm/), FSL, version 4 (fsl.fmrib.ox.ac.uk/fsl/fslwiki/), and custom MATLAB routines. Preprocessing included slice time correction, motion correction, and field map-based undistortion (59). Data were high-pass filtered, but to maintain high-spatial resolution, they were neither smoothed nor normalized (30).

Bilateral ERC and bilateral DG/CA3 (Fig. 1*A*) were defined manually for each participant in native space using established procedures (60) and were coregistered to functional space. ROIs were segmented by two raters (S.E.F. and J.D.B.) blinded to group status. Interrater reliability for a subset of six brains was evaluated by calculating Dice coefficients for each ROI; analyses indicated a mean overlap value of 0.75 for ERC and 0.72 for DG/CA3.

Time courses were extracted from each ROI and participant using MarsBaR's finite impulse response model (marsbar.sourceforge.net/). The design matrix for the encoding phase contained entries for novel pairs broken down into SII, SIR, SIN, and SR trials, as well as repeated pairs and trials with no response. The design matrix for the retrieval phase contained entries for the nine conditions described above, as well as a 10th condition for trials with no response. The underlying hemodynamic response in each ROI for each condition was estimated by averaging the signal at 2-s bins beginning at stimulus onset and ending 14 s after stimulus onset. To obtain an overall measure of activity in each ROI for each condition, integrated percent signal change was calculated by summing together signal estimates from 4- to 12-s poststimulus onset to encompass activity pertaining to both stimulus presentation and participant response.

Multiple Linear Regression. The degree to which MTL subfield structure and function can explain differences in memory was assessed using multiple linear regression. All analyses were performed using R (www.r-project.org/). Associative d' served as the dependent variable, and explanatory variables included ERC thickness, CA1-SRLM thickness, ERC activity, and DG/CA3 activity, while controlling for participant diagnostic group and age (see *SI Methods* for methods used for non-a priori ROIs). Separate models were run for encoding and retrieval data such that structural and control variables remained the same, but functional variables changed according to task phase. For the encoding model, subfield activity was defined as [SII activity] − [SIR activity], reflecting successful associative encoding. For the retrieval model, subfield activity was defined as [II activity] − [IR activity], reflecting successful associative retrieval. All explanatory variables were normalized. See *SI Results* for a test of collinearity among variables and Fig. S5 for a correlation matrix involving each variable.

Code Sharing. All custom code is posted to the Stanford Memory Lab's Github archive at https://github.com/WagnerLab/Carr_PNAS.

ACKNOWLEDGMENTS. We thank Christina Wyss-Coray and Michelle Fenesy for performing neuropsychological testing. This work was supported by grants from the National Institute of Aging (R01-AG048076), National Institute of Mental Health (F32-MH087012), National Institute of Biomedical Imaging and Bioengineering (P41-EB015891); McKnight Endowment Fund for Neuroscience; Dana Foundation; and GE Healthcare.

1. Spencer WD, Raz N (1995) Differential effects of aging on memory for content and context: A meta-analysis. *Psychol Aging* 10:527–539.
2. Craik F, Salthouse TA (2011) *The Handbook of Aging and Cognition* (Psychology Press, New York), 3rd Ed.
3. Old SR, Naveh-Benjamin M (2008) Differential effects of age on item and associative measures of memory: A meta-analysis. *Psychol Aging* 23:104–118.
4. Scoville WB, Milner B (1957) Loss of recent memory after bilateral hippocampal lesions. *J Neurol Neurosurg Psychiatry* 20:11–21.
5. Squire LR, Stark CEL, Clark RE (2004) The medial temporal lobe. *Annu Rev Neurosci* 27: 279–306.
6. Eichenbaum H, Yonelinas AP, Ranganath C (2007) The medial temporal lobe and recognition memory. *Annu Rev Neurosci* 30:123–152.
7. Preston AR, Wagner AD (2007) The medial temporal lobe and memory. *Neurobiology of Learning and Memory* (Academic Press, Burlington, MA), eds Kesner RP, Martinez JL, 2nd Ed, pp 305–337.
8. Lister JP, Barnes CA (2009) Neurobiological changes in the hippocampus during normative aging. *Arch Neurol* 66:829–833.
9. Leal SL, Yassa MA (2015) Neurocognitive aging and the hippocampus across species. *Trends Neurosci* 38:800–812.
10. Insausti R, Amaral DG (2012) Hippocampal formation. *The Human Nervous System*, eds Mai JK, Paxinos G (Academic Press, San Diego), 3rd Ed, pp 896–942.
11. de Flores R, La Joie R, Chételat G (2015) Structural imaging of hippocampal subfields in healthy aging and Alzheimer's disease. *Neuroscience* 309:29–50.
12. Mueller SG, et al. (2007) Measurement of hippocampal subfields and age-related changes with high resolution MRI at 4T. *Neurobiol Aging* 28:719–726.
13. Shing YL, et al. (2011) Hippocampal subfield volumes: Age, vascular risk, and correlation with associative memory. *Front Aging Neurosci* 3:2.
14. Raz N, Daugherty AM, Bender AR, Dahle CL, Land S (2015) Volume of the hippocampal subfields in healthy adults: Differential associations with age and a pro-inflammatory genetic variant. *Brain Struct Funct* 220:2663–2674.
15. Daugherty AM, Bender AR, Raz N, Ofen N (2016) Age differences in hippocampal subfield volumes from childhood to late adulthood. *Hippocampus* 26:220–228.
16. Dickerson BC, et al. (2009) Differential effects of aging and Alzheimer's disease on medial temporal lobe cortical thickness and surface area. *Neurobiol Aging* 30: 432–440.
17. Du A-T, et al. (2006) Age effects on atrophy rates of entorhinal cortex and hippocampus. *Neurobiol Aging* 27:733–740.
18. Thomann PA, et al. (2013) Hippocampal and entorhinal cortex volume decline in cognitively intact elderly. *Psychiatry Res* 211:31–36.
19. Raz N, Ghisletta P, Rodrigue KM, Kennedy KM, Lindenberger U (2010) Trajectories of brain aging in middle-aged and older adults: Regional and individual differences. *Neuroimage* 51:501–511.
20. Braak E, Braak H (1997) Alzheimer's disease: Transiently developing dendritic changes in pyramidal cells of sector CA1 of the Ammon's horn. *Acta Neuropathol* 93:323–325.
21. Braak H, Alafuzoff I, Arzberger T, Kretzschmar H, Del Tredici K (2006) Staging of Alzheimer disease-associated neurofibrillary pathology using paraffin sections and immunocytochemistry. *Acta Neuropathol* 112:389–404.
22. Thal DR, et al. (2000) Alzheimer-related tau-pathology in the perforant path target zone and in the hippocampal stratum oriens and radiatum correlates with onset and degree of dementia. *Exp Neurol* 163:98–110.
23. Xu Y, et al. (2000) Usefulness of MRI measures of entorhinal cortex versus hippocampus in AD. *Neurology* 54:1760–1767.
24. Killiany RJ, et al. (2002) MRI measures of entorhinal cortex vs hippocampus in preclinical AD. *Neurology* 58:1188–1196.
25. Krumm S, et al. (2016) Cortical thinning of parahippocampal subregions in very early Alzheimer's disease. *Neurobiol Aging* 38:188–196.
26. Mueller SG, et al. (2010) Hippocampal atrophy patterns in mild cognitive impairment and Alzheimer's disease. *Hum Brain Mapp* 31:1339–1347.
27. Kerchner GA, et al. (2010) Hippocampal CA1 apical neuropil atrophy in mild Alzheimer disease visualized with 7-T MRI. *Neurology* 75:1381–1387.
28. Kerchner GA, et al. (2013) Shared vulnerability of two synaptically-connected medial temporal lobe areas to age and cognitive decline: A seven tesla magnetic resonance imaging study. *J Neurosci* 33:16666–16672.
29. Leal SL, Yassa MA (2013) Perturbations of neural circuitry in aging, mild cognitive impairment, and Alzheimer's disease. *Ageing Res Rev* 12:823–831.
30. Carr VA, Rissman J, Wagner AD (2010) Imaging the human medial temporal lobe with high-resolution fMRI. *Neuron* 65:298–308.
31. Yassa MA, et al. (2011) Pattern separation deficits associated with increased hippocampal CA3 and dentate gyrus activity in nondemented older adults. *Hippocampus* 21:968–979.
32. Yassa MA, Mattfeld AT, Stark SM, Stark CEL (2011) Age-related memory deficits linked to circuit-specific disruptions in the hippocampus. *Proc Natl Acad Sci USA* 108: 8873–8878.
33. Yassa MA, et al. (2010) High-resolution structural and functional MRI of hippocampal CA3 and dentate gyrus in patients with amnestic mild cognitive impairment. *Neuroimage* 51:1242–1252.
34. Bakker A, et al. (2012) Reduction of hippocampal hyperactivity improves cognition in amnestic mild cognitive impairment. *Neuron* 74:467–474.
35. Bakker A, Albert MS, Krauss G, Speck CL, Gallagher M (2015) Response of the medial temporal lobe network in amnestic mild cognitive impairment to therapeutic intervention assessed by fMRI and memory task performance. *Neuroimage Clin* 7: 688–698.
36. Daselaar SM, Fleck MS, Dobbins IG, Madden DJ, Cabeza R (2006) Effects of healthy aging on hippocampal and rhinal memory functions: An event-related fMRI study. *Cereb Cortex* 16:1771–1782.
37. Cabeza R, et al. (2004) Task-independent and task-specific age effects on brain activity during working memory, visual attention and episodic retrieval. *Cereb Cortex* 14:364–375.
38. Dulas MR, Duarte A (2012) The effects of aging on material-independent and material-dependent neural correlates of source memory retrieval. *Cereb Cortex* 22: 37–50.
39. Persson J, et al. (2012) Longitudinal structure-function correlates in elderly reveal MTL dysfunction with cognitive decline. *Cereb Cortex* 22:2297–2304.
40. Huijbers W, et al. (2014) Amyloid deposition is linked to aberrant entorhinal activity among cognitively normal older adults. *J Neurosci* 34:5200–5210.
41. Dickerson BC, et al. (2005) Increased hippocampal activation in mild cognitive impairment compared to normal aging and AD. *Neurology* 65:404–411.
42. Davachi L (2006) Item, context and relational episodic encoding in humans. *Curr Opin Neurobiol* 16:693–700.
43. Mueller SG, Chao LL, Berman B, Weiner MW (2011) Evidence for functional specialization of hippocampal subfields detected by MR subfield volumetry on high resolution images at 4 T. *Neuroimage* 56:851–857.
44. Fouquet M, et al. (2012) Role of hippocampal CA1 atrophy in memory encoding deficits in amnestic mild cognitive impairment. *Neuroimage* 59:3309–3315.
45. Kerchner GA, et al. (2012) Hippocampal CA1 apical neuropil atrophy and memory performance in Alzheimer's disease. *Neuroimage* 63:194–202.
46. Jagust W (2013) Vulnerable neural systems and the borderland of brain aging and neurodegeneration. *Neuron* 77:219–234.
47. Alzheimer's Association (2016) 2016 Alzheimer's disease facts and figures. *Alzheimers Dement* 12:459–509.
48. Villemagne VL, et al.; Australian Imaging Biomarkers and Lifestyle (AIBL) Research Group (2013) Amyloid β deposition, neurodegeneration, and cognitive decline in sporadic Alzheimer's disease: A prospective cohort study. *Lancet Neurol* 12:357–367.
49. Braak H, Braak E (1997) Frequency of stages of Alzheimer-related lesions in different age categories. *Neurobiol Aging* 18:351–357.
50. Mizutani T, Kasahara M (1997) Hippocampal atrophy secondary to entorhinal cortical degeneration in Alzheimer-type dementia. *Neurosci Lett* 222:119–122.
51. Scheff SW, Price DA, Schmitt FA, DeKosky ST, Mufson EJ (2007) Synaptic alterations in CA1 in mild Alzheimer disease and mild cognitive impairment. *Neurology* 68:1501–1508.
52. Boutet C, et al. (2014) Detection of volume loss in hippocampal layers in Alzheimer's disease using 7 T MRI: A feasibility study. *Neuroimage Clin* 5:341–348.
53. Sperling RA, et al. (2010) Functional alterations in memory networks in early Alzheimer's disease. *Neuromolecular Med* 12:27–43.
54. de Chastelaine M, Mattson JT, Wang TH, Donley BE, Rugg MD (2016) The neural correlates of recollection and retrieval monitoring: Relationships with age and recollection performance. *Neuroimage* 138:164–175.
55. Hashimoto M, Masliah E (2003) Cycles of aberrant synaptic sprouting and neurodegeneration in Alzheimer's and dementia with Lewy bodies. *Neurochem Res* 28:1743–1756.
56. Stern EA, et al. (2004) Cortical synaptic integration in vivo is disrupted by amyloid-beta plaques. *J Neurosci* 24:4535–4540.
57. Ebner NC (2008) Age of face matters: Age-group differences in ratings of young and old faces. *Behav Res Methods* 40:130–136.
58. Sperling RA, et al. (2003) fMRI studies of associative encoding in young and elderly controls and mild Alzheimer's disease. *J Neurol Neurosurg Psychiatry* 74:44–50.
59. Jezzard P, Balaban RS (1995) Correction for geometric distortion in echo planar images from B0 field variations. *Magn Reson Med* 34:65–73.
60. Olsen RK, et al. (2009) Performance-related sustained and anticipatory activity in human medial temporal lobe during delayed match-to-sample. *J Neurosci* 29:11880–11890.
61. Morris JC (1993) The clinical dementia rating (CDR): Current version and scoring rules. *Neurology* 43:2412–2414.
62. Cummings JL, et al. (1994) The neuropsychiatric inventory: Comprehensive assessment of psychopathology in dementia. *Neurology* 44:2308–2314.
63. Sheikh JI, Yesavage JA (1986) Geriatric depression scale (GDS): Recent evidence and development of a shorter version. *Clinical Gerontology: A Guide to Assessment and Intervention* (The Haworth Press, New York), pp 165–173.
64. Pfeffer RI, Kurosaki TT, Harrah CH (1982) Measurement of functional activities in older adults in the community. *J Gerontol* 37:323–329.
65. Albert MS, et al. (2011) The diagnosis of mild cognitive impairment due to Alzheimer's disease: Recommendations from the National Institute on Aging-Alzheimer's Association workgroups on diagnostic guidelines for Alzheimer's disease. *Alzheimers Dement* 7:270–279.
66. Brandt J (1991) The hopkins verbal learning test: Development of a new memory test with six equivalent forms. *Clin Neuropsychol* 5:125–142.
67. Benedict RH (1997) *Brief Visuospatial Memory Test-Revised* (Psychological Assessment Resources, Odessa, FL).
68. Wechsler D (1997) *Wechsler Memory Scale* (The Psychological Corporation, San Antonio, TX), 3rd Ed.